Simple and improved approach of estimating MIMO capacity from antenna magnitude patterns

Tian, Ruiyuan; Lau, Buon Kiong

Published in:
3rd European Conference on Antennas and Propagation, EuCAP 2009.

2009

Document Version:
Peer reviewed version (aka post-print)

Link to publication

Citation for published version (APA):
Tian, R., & Lau, B. K. (2009). Simple and improved approach of estimating MIMO capacity from antenna magnitude patterns. In *3rd European Conference on Antennas and Propagation, EuCAP 2009.* (pp. 1770-1774). IEEE - Institute of Electrical and Electronics Engineers Inc.. https://ieeexplore.ieee.org/stamp/stamp.jsp?tp=&arnumber=5067977

Total number of authors:
2

Simple and Improved Approach of Estimating MIMO Capacity from Antenna Magnitude Patterns

Ruiyuan Tian [1] and Buon Kiong Lau [2]

Department of Electrical and Information Technology
Lund University, Sweden
[1]ruiyuan@eit.lth.se, [2]bkl@eit.lth.se

Abstract— **This paper proposes a simple and improved approach of estimating MIMO capacity from antenna magnitude patterns, *i.e.*, the antenna patterns are phaseless. The simple approach synthesizes the phases according to the antenna spacing, and it compares favorably with an existing approach based on random phase synthesis. Moreover, the simple approach can be improved by taking into account the correlation between the magnitude patterns. The performance of the existing and proposed approaches in estimating MIMO capacity is investigated for dipole antenna systems with different gain and correlation characteristics, under different conditions of antenna spacings, impedance matching networks and propagation scenarios. It is found that an average capacity estimation error of under 0.5% is achieved for the proposed approach, as compared to up to 20.6% error for the random phase approach.**

I. Introduction

Multiple antenna systems have been proposed as a promising technique to achieve high spectrum efficiency in wireless communications. Such systems perform best when the spatial correlation among signals on different antenna branches is low [1]. Therefore, the implementation of a compact multiple antenna system is very challenging, since multiple antenna elements need to be closely spaced, which leads to both high correlation between received signals and high electromagnetic mutual coupling (MC) among antenna elements. Recent work has shown that matching networks have a significant influence on this problem. For example, optimal performance on signal correlation [2], diversity [3] and capacity [4] can be achieved at the cost of narrower bandwidth [5], if a sophisticated multiport matching network is utilized.

On the other hand, one convenient approach to evaluate the performance of MIMO systems relies on the accurate measurement of complex antenna radiation patterns for all antenna elements (see *e.g.*, [4]). However, phase information is usually not available in active measurements of mobile terminals [6]. Instead, one can for example apply a phase-retrieval-capable antenna measurement system [7], which has the penalty of adding complexity to the testing equipment/procedure. Effects of phaseless (or magnitude only) patterns on MIMO performance have been evaluated in [8], in which the results show that the use of phaseless antenna patterns leads to unacceptably large underestimation of MIMO performance. Nevertheless, it is demonstrated that adding random phases to phaseless patterns can help to reduce the estimation errors [8]. The study of [8] is based on the evaluation of five antenna prototypes with a fixed antenna spacing for each prototype.

In this paper, an end-to-end MIMO system using antenna arrays with two dipole antennas is investigated. The discussion in [8] is extended in that the impact of phaseless antenna patterns on MIMO performance is investigated for the whole continuum of small antenna spacings, taking into account the use of different matching networks which modify the pattern phases. In this context, a new phase synthesis approach for improving the estimation of MIMO performance based on magnitude patterns is proposed: we begin with a simple approach that synthesizes phases according to the antenna spacing, and this is followed by an improved version that adjusts the randomness of the synthesized phases according to the magnitude pattern correlation. The performance of the two variants of the new approach is evaluated and compared to the random phase approach in [8]. Different propagation scenarios with uniform angular power spectrum (APS) and limited angular spread in the azimuth plane (*i.e.*, elevation spread is neglected) are considered in the study.

We begin with a presentation of the system model and evaluation framework in Sections II and III. Next, the results and discussions are given in Section IV. Finally, we make some concluding remarks in Section V.

II. System Model

In this section, the system model will be established, with a focus on the receive (RX) subsystem. In this study, uniform linear arrays (ULAs) of two half-wavelength ($\lambda/2$) dipoles with the diameter of $\lambda/400$ are considered. Antenna parameters are obtained through method of moments (MoM) [9] simulations, as in [5].

A. Receive Subsystem

The RX subsystem consists of coupled RX antennas, a matching network, and load impedances. The block diagram of the RX subsystem is shown in Figure 1. Specifically, in a 2×2 MIMO system, $\mathbf{Z}_{\mathrm{RR}}$ is a 2×2 antenna impedance matrix whose diagonal and off-diagonal elements represent the self- and mutual-impedances, respectively, so that mutual coupling is considered. Z_{L1} and Z_{L2} are the load impedances for ports 1 and 2, respectively.

This work was supported by VINNOVA (Grant no. 2007-01377) and Vetenskapsradet (Grant no. 2006-3012).

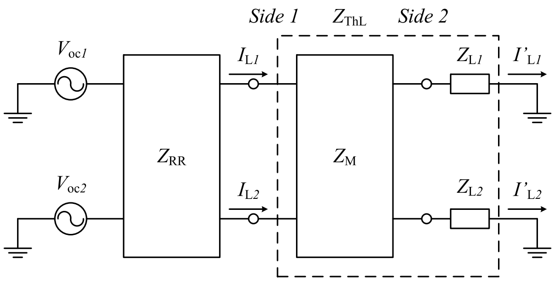

Fig. 1. Block diagram of a 2×2 MIMO RX subsystem.

The matching network is denoted by $\mathbf{Z}_{\rm M}$, which represents a 4×4 matching network matrix in the system with the matrix structure of

$$\mathbf{Z}_{\rm M} = \begin{bmatrix} \mathbf{Z}_{11} & \mathbf{Z}_{12} \\ \mathbf{Z}_{21} & \mathbf{Z}_{22} \end{bmatrix}. \quad (1)$$

In this work, several different matching conditions are discussed, including characteristic impedance match, self impedance match, input impedance match (which are single port match) and multiport conjugate match. These matching conditions for multiple antenna systems have been discussed extensively in [2]–[5].

B. Transmit Subsystem

The transmit (TX) subsystem contains similar components as in the RX subsystem, where "Side 1" of the matching network is connected to the TX antennas while "Side 2" is connected to the sources.

C. Circuit Model

In the RX subsystem, the excitation sources are the open-circuit voltages $\boldsymbol{V}_{\rm oc} = [V_{\rm oc1}, V_{\rm oc2}]^T$. The currents induced at the input of matching networks $\boldsymbol{I}_{\rm L} = [I_{\rm L1}, I_{\rm L2}]^T$ can be obtained as

$$\boldsymbol{I}_{\rm L} = (\mathbf{Z}_{\rm RR} + \mathbf{Z}_{\rm ThL})^{-1}\boldsymbol{V}_{\rm oc}, \quad (2)$$

in which $\mathbf{Z}_{\rm ThL}$ denotes the Thevenin equivalent load impedance as seen by the antenna ports, and it is given by

$$\mathbf{Z}_{\rm ThL} = \mathbf{Z}_{11} - \mathbf{Z}_{12}(\mathbf{Z}_{\rm L} + \mathbf{Z}_{22})^{-1}\mathbf{Z}_{21}. \quad (3)$$

The output voltages over the load impedances are found as

$$\boldsymbol{V}'_{\rm L} = \mathbf{Z}_{\rm L}\boldsymbol{I}'_{\rm L} = \mathbf{Z}_{\rm L}(\mathbf{Z}_{22} + \mathbf{Z}_{\rm L})^{-1}\mathbf{Z}_{21}\boldsymbol{I}_{\rm L}. \quad (4)$$

Substituting (2) into (4) gives us the transfer function between the open-circuit voltages and the output voltages,

$$\boldsymbol{V}'_{\rm L} = \mathbf{Z}_{\rm L}(\mathbf{Z}_{22} + \mathbf{Z}_{\rm L})^{-1}\mathbf{Z}_{21}(\mathbf{Z}_{\rm RR} + \mathbf{Z}_{\rm ThL})^{-1}\boldsymbol{V}_{\rm oc}. \quad (5)$$

D. Channel Model

A path-based channel model is used to represent the propagation part of the complete MIMO system [4]. In our case, the model is represented by a trans-impedance matrix relating the output voltages at the open-circuited RX antenna ports $\boldsymbol{V}_{\rm oc}$ to the excitation current at each of the TX antenna ports, with the other ports open-circuited. For the channel between the j-th TX antenna and the i-th RX antenna $\mathbf{H}(i,j)$, the trans-impedance $\mathbf{Z}_{{\rm RT},ij}$ for the single polarization case can be described as

$$\mathbf{Z}_{{\rm RT},ij} = \sum_{n=1}^{N} E_i^{\rm R}(\theta_n^{\rm R}, \varphi_n^{\rm R})\beta(\theta_n^{\rm R}, \varphi_n^{\rm R}, \theta_n^{\rm T}, \varphi_n^{\rm T})e_j^{\rm T}(\theta_n^{\rm T}, \varphi_n^{\rm T}), \quad (6)$$

in which N is the total number of TX-RX paths, $(\theta_n^{\rm R}, \varphi_n^{\rm R})$ and $(\theta_n^{\rm T}, \varphi_n^{\rm T})$ represent the elevation and azimuth angle of arrival (AoA) and angle of departure (AoD) of the n-th path, respectively. $E_i^{\rm R}(\theta_n^{\rm R}, \varphi_n^{\rm R})$ is the complex pattern for the i-th RX antenna (with all ports open-circuited), while $e_j^{\rm T}(\theta_n^{\rm T}, \varphi_n^{\rm T})$ is the field per unit source current of the j-th TX antenna (with all ports open-circuited, except the j-th port) [4]. $\beta(\theta_n^{\rm R}, \varphi_n^{\rm R}, \theta_n^{\rm T}, \varphi_n^{\rm T})$ describes channel gain of the n-th path, which can be statistically characterized by the given APS at both the TX and RX ends.

III. Evaluation Framework

A. System Configurations

In order to facilitate comparison, a reference end-to-end MIMO system is set up. In the reference TX subsystem, antennas are assumed to have no mutual coupling (only spatial correlation exists) and the self impedance match is employed at each antenna port. The reference RX subsystem is set to the same configurations, *i.e.*, no mutual coupling between the reference RX antennas and self impedance match is employed at each RX antenna port. The list of all system configurations considered in this work is given in Table I.

B. Propagation Scenarios

In this study, antenna patterns with both polarizations are investigated in the azimuth plane ($\theta = \pi/2$). A uniform 2D APS is assumed on the TX side. On the RX side, however, two different APS are considered. In one case, the APS is of a uniform 2D distribution, whereas in the other case it is of a Laplacian 2D distribution with limited angular spread, *i.e.*, standard deviation of 30° centered at the array broadside [10].

C. Performance Metrics

Output correlation and channel capacity are used to characterize MIMO performance over the whole continuum of small antenna spacings in the RX side. The TX antenna spacing is, however, fixed to $d = \lambda$ for the sake of simple comparison with no loss of generality.

TABLE I
List of system configurations.

		Mutual Coupling	Matching Network Type
TX		No	Self impedance
RX	Ref	No	Self impedance
	S1	Yes	Characteristic impedance
	S2	Yes	Self impedance
	S3	Yes	Input impedance
	S4	Yes	Multiport conjugate [2]
	S5	Yes	Multiport conjugate [4]

The output correlation is calculated from the APS of the propagation environment and the antenna patterns taken at the output or "Side 2" of the matching network (see Figure 1) [11]. In this case, only the RX subsystem is considered.

The capacity calculation is based on MIMO channel matrices that are obtained using the channel model discussed in Section II-D, with $N = 360$. In total, 10000 channel realizations are generated according to the given TX/RX APS. The channel matrices obtained for RX subsystems with mutual coupling and different matching networks (S1-S5) are then normalized against the reference system (Ref) (see Table I), so that the matched antenna efficiency is accounted for. The 10% outage capacity without channel knowledge at the TX subsystem for SNR of $20\,\mathrm{dB}$ is numerically evaluated.

D. Evaluation Cases

The following evaluation cases are considered for the RX antenna output patterns (*i.e.*, antenna patterns obtained at the load impedances).

1) Complex patterns: When the complex patterns are present, *i.e.*, full magnitude and phase information is available, the resulting capacity reflects the actual system performance. The other cases are evaluated with respect to this performance.

2) Magnitude patterns: The antenna output patterns are phaseless, *i.e.*, only the magnitude patterns are available [6].

3) Random-phase patterns: In order to compensate for the underestimation of capacity due to the absence of phase information, uniformly distributed random phases $\varphi \in (-\pi, \pi]$ can be added to the magnitude patterns [8].

4) Phase-synthesis patterns: When the antenna spacing d is known, one can apply the array steering vector as a simple method for phase synthesis. For example, in the 2D case where the phase center is situated at the broadside of the ULA with two identical and parallel dipole elements, the phases on the antennas due to the impinging waves with azimuth AoAs $\boldsymbol{\varphi}$ are obtained as

$$\mathbf{a} = \left[\mathrm{e}^{-j\pi \frac{d}{\lambda} \cos \boldsymbol{\varphi}}, \mathrm{e}^{j\pi \frac{d}{\lambda} \cos \boldsymbol{\varphi}} \right]^T, \tag{7}$$

where λ denotes the wavelength of the signal.

However, these phases can be changed significantly due to the influence of mutual coupling and matching networks that are employed. We propose to account for this influence on phase by adding a degree of randomness to the synthesized phases that depends on the correlation of the magnitude patterns. To accomplish this, the synthesized phases are modified as

$$\mathbf{a}' = \mathbf{R} \odot \mathbf{a}, \tag{8}$$

where $\odot$ denotes element wise multiplication. $\mathbf{R}$ is a correlation matrix which is obtained through correlating two random sequences $\boldsymbol{c}_1$ and $\boldsymbol{c}_2$ as

$$\mathbf{R} = \begin{bmatrix} 1 & \alpha \\ \alpha^* & 1 \end{bmatrix} \begin{bmatrix} \boldsymbol{c}_1 \\ \boldsymbol{c}_2 \end{bmatrix}. \tag{9}$$

where $\boldsymbol{c}_1, \boldsymbol{c}_2 \in \mathbb{C}^{1\times N}$ and are independent and identically distributed with zero mean circularly symmetric complex

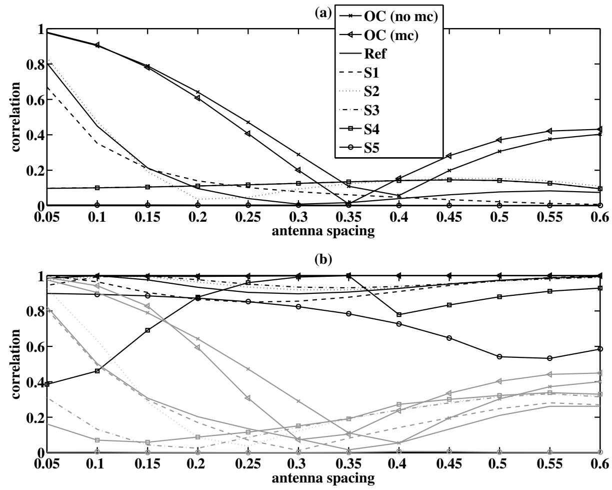

Fig. 2. Output correlation versus antenna spacing (in wavelength unit) with uniform 2D APS. Curves in the top figure show the correlation of complex output patterns with different system configurations. Darker and lighter curves in the bottom figure correspond to correlation of magnitude-only and phase-only patterns, respectively.

Gaussian random variables. The role of α is to scale the correlation (or randomness) of the synthesized phases, and it is obtained from the available magnitude pattern correlation r_m,

$$\alpha = \zeta r_\mathrm{m}, \tag{10}$$

where ζ is a factor that can be adjusted for a given propagation scenario.

IV. Results

A. Output Correlation

RX output correlations obtained with a uniform 2D APS are shown in Figure 2 for different system configurations. Matching networks can reduce the correlation significantly, and low correlation can be obtained for any antenna spacings when a sophisticated matching network (S3, S4 or S5) is employed. According to the results, the correlation of phase-only patterns behaves more similarly as the correlation of complex patterns. This highlights the importance of phase information in the output antenna patterns. On the other hand, the output correlation obtained from the magnitude-only patterns is high in general, which leads to the underestimation of MIMO performance. Nevertheless, it is also observed that a lower magnitude correlation tends to indicate a lower correlation in the complex patterns, especially for small antenna spacings. This shows that we can try to use magnitude correlation as additional phase synthesis information for improving the estimation of capacity when only magnitude patterns are available.

B. MIMO Capacity

Figure 3 shows the channel capacity versus antenna spacing for different system configurations and two propagation scenarios when complex patterns are available. When only

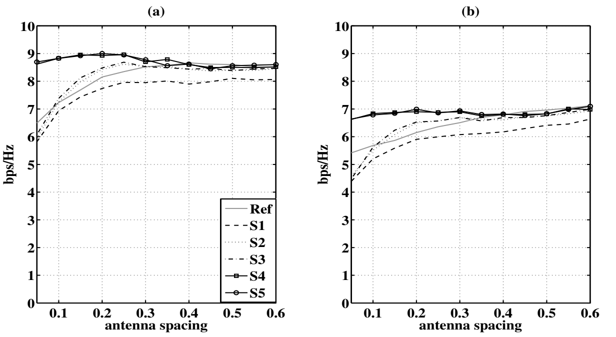

Fig. 3. 10% outage capacity versus antenna spacing (in wavelength unit). (a) Uniform 2D APS; (b) Laplacian 2D APS.

the magnitude patterns are available, one should consider the alternative evaluation cases that are discussed in Section III-D. The estimated MIMO capacity from each evaluation case is compared to the results in Figure 3 and the corresponding estimation error is obtained.

In Table II, the estimation error of each case is averaged over different system configurations (S1-S5), as well as over the small antenna spacings of $0.05\lambda \leq d \leq 0.5\lambda$, for uniform and Laplacian 2D APS, respectively. The results are expressed in percentage error with respect to the 10% outage channel capacity in bps/Hz that is obtained when the complex output patterns are present. "$+$" denotes overestimated capacity whereas "$-$" denotes underestimated capacity. This average measure gives a quick indication of the overall estimation performance of each evaluation case.

To give more details of the error performance, subplots in Figure 4 illustrate the estimation error over the antenna spacing and system configurations S1 to S5 for the random-phase patterns, simple and improved phase-synthesis patterns using phase vector $\boldsymbol{a}$ and $\boldsymbol{a}'$, respectively:

1) Complex pattern: The capacity performance in Figure 3 reflects the actual system performance. As shown in Figure 3a for the case of uniform 2D APS, the capacity of the reference system (Ref) increases with increasing antenna spacing due to decreasing output correlation, and stabilizes around $d = 0.3\lambda$, when the correlation is low enough so that it is no longer the dominant influence. Matched antenna systems (S1-S5) exhibit differences in capacity performance relative to Ref due to their respective behavior in both power loss (efficiency) and

TABLE II

AVERAGE PERFORMANCE ON MIMO CAPACITY ESTIMATION BASED ON DIFFERENT EVALUATION CASES WITH (1) UNIFORM 2D APS (UNI); (2) LAPLACIAN 2D APS (LAP).

	UNI	LAP
Magnitude	-19.6%	-12.7%
Random-phase	+2.2%	+20.6%
Simple phase-synthesis $\boldsymbol{a}$	-3.2%	-2.1%
Improved phase-synthesis $\boldsymbol{a}'$	-0.5%	-0.3%

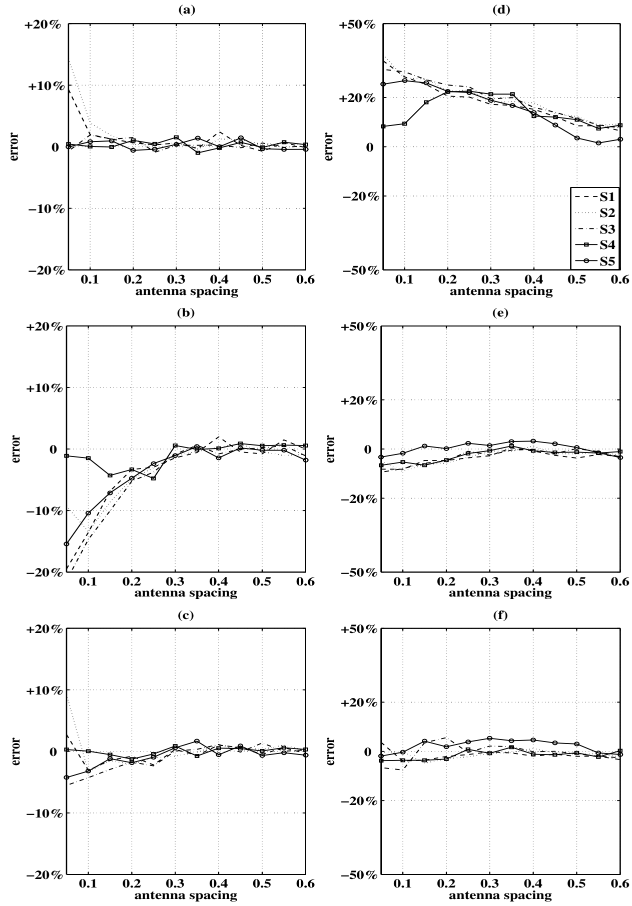

Fig. 4. Estimation error on MIMO capacity versus antenna spacing (in wavelength unit), with (i) uniform 2D APS: (a) Random-phase pattern, (b) Simple phase-synthesis pattern, (c) Improved phase-synthesis pattern; (ii) Laplacian 2D APS: (d) Random-phase pattern, (e) Simple phase-synthesis pattern, (f) Improved phase-synthesis pattern.

output correlation. In particular, when the multiport matching networks (S4 and S5) are employed, even with very small antenna spacings, good capacity performance can still be obtained, which is partly due to the very low output correlation of the system (see Figure 2). Moreover, as pointed out in [4] and [5], the RX antennas in S4 and S5 are also perfectly matched (*i.e.*, no loss of efficiency due to self-reflection or coupling).

When the APS is of limited angular spread, *e.g.*, a Laplacian 2D APS, the output patterns are highly correlated so that a poorer capacity performance is obtained as shown in Figure 3b.

2) Magnitude pattern: Magnitude patterns result in a high output correlation which leads to a low channel capacity. This is confirmed in Table II where the MIMO capacity is unacceptably underestimated.

3) Random-phase pattern: Random phases are added to the magnitude patterns to mitigate the aforementioned capacity underestimation. As can be seen in Figure 4a, this approach generally offer a good capacity estimation performance in a propagation environment with uniform APS. However, since random phases maximize phase diversity without considering the environment or the antenna systems, it can lead to an overestimated performance. As can be seen in Figure 4a for small antenna spacings ($d \leq 0.1\lambda$), capacity overestimation is observed for systems S1 and S2, whereas the estimation error is negligible for S3, S4 and S5. This can be interpreted by the very low phase correlations of S3, S4 and S5 which enable random phases to offer good approximation.

On the other hand, when the propagation environment is with Laplacian 2D APS, the output patterns are more highly correlated than the uniform 2D case and thus bear less resemblance to random phases. Figure 4d clearly shows that random-phase patterns lead to significant overestimation.

4) Simple phase-synthesis pattern: The synthesized phases according to the array steering vector $\boldsymbol{a}$ should be precise if neither mutual coupling nor matching networks are considered, since these two factors can change the phases in $\boldsymbol{a}$ significantly. However, as indicated by Table II and Figure 4b, it leads to underestimated capacity when these effects are taken into account in S1-S5. The errors are reduced for the propagation environment with Laplacian 2D APS (see Figure 4e), since in this case the spatial correlation as described by the array steering vector dominates the performance.

5) Improved phase-synthesis pattern: Using some trials and errors, appropriate values of ζ in (10) are found to be 0.5 and 0.9 for the propagation environment with uniform and Laplacian 2D APS, respectively. One can also optimize ζ by formulating the capacity estimation problem as an optimization problem. In Table II, it can be seen that the improved phase-synthesis method using the phase vector $\boldsymbol{a}'$ achieves the best overall performance. It achieves a good balance between the overestimation resulted from the random phases and the underestimation resulted from the simple synthesized phases by adding a degree of randomness to the steering vector according to the correlation of magnitude patterns.

C. Discussions

The above study shows that magnitude-only patterns result in unacceptably large estimation errors of MIMO capacity performance for both uniform and Laplacian 2D APS. This finding is consistent with the results in [8], which indicates that channel capacity is significantly underestimated when the phase information of the output patterns is unavailable. Therefore, phases should be synthesized in a manner as to mitigate the capacity underestimation. Additionally, different matching networks in the antenna system have been shown to change the phases significantly, which then produce different correlation characteristics in the output patterns.

The random-phase approach simply adds random phases to the magnitude patterns. With uniform APS and small antenna spacings, random-phase patterns provide good performance estimation for antenna systems with sophisticated matching networks (S3-S5) in which the phase correlation is characteristically low due to the matching networks. However, it exhibits overestimated performance in simple matched systems (S1 or S2) for uniform 2D APS and in systems S1-S5 for Laplacian 2D APS. This is because in these cases the actual phase correlation is higher than what random phases can offer.

On the other hand, the simple phase-synthesis patterns result in capacity underestimation for small antenna spacings in all the systems S1-S5. Therefore, an improved phase-synthesis method is proposed in which the magnitude pattern correlation is used to add a degree of randomness to the steering vector phases. The results indicate that significantly more accurate capacity estimation performance is achieved over all the investigated parameters using the improved phase-synthesis patterns.

V. Conclusions

This paper focused on the estimation of MIMO capacity performance with synthesized antenna output patterns, and different impedance matching networks, antenna spacings and propagation scenarios are considered to provide a wide range of correlation characteristics. The proposed phase-synthesis approach using the array steering vector as well as the magnitude pattern correlation has been found to give significantly better performance than the existing random phase approach for all the investigated parameters.

Acknowledgment

Helpful discussions with Dr Joonas Krogerus of Nokia Research Center, Helsinki, Finland is gratefully acknowledgment.

References

[1] M. Jensen and J. Wallace, "A review of antennas and propagation for mimo wireless communications," *IEEE Transactions on Antennas and Propagation*, vol. 52, no. 11, pp. 2810–2824, Nov. 2004.

[2] S. Dossche, S. Blanch, and J. Romeu, "Optimum antenna matching to minimise signal correlation on a two-port antenna diversity system," *Electronics Letters*, vol. 40, no. 19, pp. 1164–1165, Sep. 2004.

[3] J. Wallace and M. Jensen, "Termination-dependent diversity performance of coupled antennas: network theory analysis," *IEEE Transactions on Antennas and Propagation*, vol. 52, no. 1, pp. 98–105, Jan. 2004.

[4] ——, "Mutual coupling in mimo wireless systems: a rigorous network theory analysis," *IEEE Transactions on Wireless Communications*, vol. 3, no. 4, pp. 1317–1325, Jul. 2004.

[5] B. K. Lau, J. B. Andersen, G. Kristensson, and A. F. Molisch, "Impact of matching network on bandwidth of compact antenna arrays," *IEEE Transactions on Antennas and Propagation*, vol. 54, no. 11, pp. 3225–3238, Nov. 2006.

[6] J. Krogerus and C. Icheln, "Considerations on anechoic chamber test methods for performance evaluation of multi-antenna mobile terminals," in *COST 2100*, TD(08) 470, Wroclaw, Poland, Feb. 6-8, 2008.

[7] T. Laitinen, J. Toivanen, C. Icheln, and P. Vainikainen, "Spherical measurement system for determination of complex radiation patterns of mobile terminals," *Electronics Letters*, vol. 40, no. 22, pp. 1392–1394, Oct. 2004.

[8] J. Krogerus, P. Suvikunnas, C. Icheln, and P. Vainikainen, "Evaluation of diversity and mimo performance of antennas from phaseless radiation patterns," in *First European Conference on Antennas and Propagation, (EuCAP 2006)*, Nov. 6-10, 2006.

[9] S. N. Makarov, *Antenna and EM modeling with MATLAB*. New York: Wiley-Interscience, 2002.

[10] A. F. Molisch, *Wireless Communications*. Wiley-IEEE Press, 2005.

[11] R. Vaughan and J. Andersen, "Antenna diversity in mobile communications," *IEEE Transactions on Vehicular Technology*, vol. 36, no. 4, pp. 149–172, Nov. 1987.